

RESEARCH

Open Access



Determination of thermal properties of grouting materials for borehole heat exchangers (BHE)

Anna Albers^{1*} , Petra Huttenloch², Roman Zorn², Hagen Steger¹ and Philipp Blum¹

*Correspondence:
anna.albers@kit.edu

¹ Institute of Applied Geosciences (AGW), Karlsruhe Institute of Technology (KIT), Kaiserstraße 12, 76131 Karlsruhe, Germany

² European Institute for Energy Research (EIFER), Emmy-Noether-Straße 11, 76131 Karlsruhe, Germany

Abstract

Thermal properties of grouting materials for borehole heat exchangers (BHE) are currently analysed with varying measurement methods and analysis procedures, resulting in difficulties when comparing values of different studies. This study therefore provides the first comprehensive investigation of different analysis procedures by systematically comparing the influence of the measurement method and the sample preparation on the determination of the thermal conductivity and the volumetric heat capacity. Seven dissimilar grouting materials with varying water–solid ratios (W/S) and compositions are analysed. The thermal conductivities of the materials range between 0.9 and 1.8 W m⁻¹ K⁻¹ (transient plane source method, TPS). The volumetric heat capacities range between 3.01 and 3.63 MJ m⁻³ K⁻¹ (differential scanning calorimetry, DSC). From the findings of this study, a standardised analysis of grouting materials is provided which suggests mixing of the grouting material at a high mixing speed and sample curing under water for 28 days at room temperature. The benefits of calculating the volumetric heat capacities of grouting materials from the specific heat capacities of dry samples measured with the DSC, the water content and the bulk density are demonstrated. Furthermore, an estimation procedure of volumetric heat capacity from the W/S and suspension density with an uncertainty of smaller ± 5% is provided. Finally, this study contributes to consistency and comparability between existing and future studies on the thermal properties of grouting materials.

Keywords: Backfill material, Borehole heat exchanger (BHE), Differential scanning calorimetry (DSC), Thermal conductivity, Volumetric heat capacity

Introduction

For the planning and design of ground source heat pump (GSHP) systems, knowledge of the thermal properties of the borehole heat exchanger (BHE) system is essential. This includes not only the thermal properties of the ground but also of the backfill material. A large number of boreholes are backfilled with grouting material (IEA ECES 2020). Reviews of grouting materials and their influence on the performance of GSHP systems are provided by Javadi et al. (2018) and Mahmoud et al. (2021). For an efficient GSHP system, high thermal conductivities λ [W m⁻¹ K⁻¹] and high volumetric heat capacities ρc_p [MJ m⁻³ K⁻¹] of the ground and backfill material are desirable. A high thermal

conductivity of the grouting material decreases the thermal borehole resistance and ensures an efficient heat transfer from the ground to the heat transfer fluid (Allan and Kavanaugh 1999; Delaleux et al. 2012; Viccaro 2018). The knowledge of the volumetric heat capacity is essential for estimating the radius of the temperature disturbance during operation and thus, evaluating the interactions with neighbored BHE (Zhou et al. 2018). Commercially available grouting materials for BHE are typically specified with a value for thermal conductivity; however, information on the volumetric heat capacity of grouting materials is often not provided. Commonly, the volumetric heat capacity is not specifically considered, as the thermal conductivity has a higher influence on the efficiency of the BHE, although the volumetric heat capacity is especially relevant at the start of the operation or when operating the BHE in intermittent mode (Li et al. 2019; Nian and Cheng 2018; Wang et al. 2022).

Albeit with the ASTM D5334-22a (ASTM International 2023) and the ASTM D4611 (ASTM International 2016), there are some standards for the measurement of thermal conductivities and specific heat capacities of soils and rocks, there is yet no standard for the analysis of the thermal properties of grouting materials. Hence, for the determination of the thermal conductivity of grouting materials, various measurement methods were applied in the literature (e.g. Delaleux et al. 2012; Erol and François 2014; Song et al. 2019). In the supporting information, a comprehensive overview of applied measurement methods is provided (Table A-1). Although some authors applied steady-state methods, where a constant temperature gradient within the sample is established (e.g. Song et al. 2019), transient methods were applied more often. The transient hot wire method (THW) was applied using a needle probe (e.g. Blázquez et al. 2017; Erol and François 2014; Kim and Oh 2020). The needle probe was inserted into the sample via holes, which can cause an underestimation of the thermal conductivity due to insufficient thermal contact between the probe and the sample (Kim and Oh 2020). Others used a surface probe, where the needle was pressed against the surface of the sample (e.g. Allan 1997; Frac et al. 2021; Kim and Oh 2020; Viccaro 2018). In some studies, the transient plane source method (TPS) was applied (e.g. Delaleux et al. 2012; Dong et al. 2022; Zhao et al. 2024). While the steady-state methods generally produce more accurate results, the transient methods have the advantage of shorter measurement times (Zhao et al. 2016). This reduces the errors due to evaporation or convection when measuring grouting materials at saturated or partly saturated conditions. Rarely, different measurement methods were compared with each other (Kim and Oh 2020). Thermal conductivity measurements were usually conducted at room temperature at about 20 °C.

Compared to the number of studies on the determination of thermal conductivity of grouting materials, there are only a few studies on the determination of volumetric heat capacity (supporting information, Table A-2). Some studies used the volumetric heat capacity values derived from transient thermal conductivity measurements (e.g. Kim and Oh 2019; Frac et al. 2021). Extremera-Jiménez et al. (2021) determined the specific heat capacity by applying the calorimetry method. The differential scanning calorimetry (DSC) method was applied to measure the specific heat capacity of dry cementitious materials based on the DIN EN ISO 11357-4 (Deutsche Norm 2021a; b) for plastics (Schutter and Taerwe 1995; Shafiq et al. 2020). Specific heat capacity values were typically provided for 20 °C, i.e. room temperature.

However, the measurement of the thermal parameters is only the last step in the analysis of grouting materials. Beforehand, the sample has to be manufactured and prepared for the measurement. Sample preparation procedures can significantly influence the results of a measurement. Sample preparation procedures of grouting materials, especially regarding the mixing and storing conditions, vary immensely between the different studies (supporting information, Table A-3). The German standard DIN EN 196-1 (Deutsche Norm 2016a) establishes the sample preparation method of cements and mortars for the analysis of the strength of cement. In some of the studies on grouting materials, these were also adapted (Frąc et al. 2021; Mascarin et al. 2022; Viccaro 2018). In analysing grouting materials, the samples have to be first manufactured by mixing the powdery raw material with a defined amount of water. The mixing procedure (including the size of the mixing vessel and the suspension volume) differed between the different studies as well as the used mixing device, which varied from disperser or mortar mixer to colloidal mixer (e.g. Allan 1997; Mascarin et al. 2022; Pascual-Muñoz et al. 2018; Viccaro 2018). After mixing, the suspension is filled in moulds and stored for curing until the measurement. Here, the specific material properties of cementitious materials have to be considered, as cementitious samples change their structure and mineralogical composition during ageing in the process of hydration (e.g. Kurdowski 2014). The samples were predominantly cured at room temperature (about 20 °C) under water (e.g. Allan 1997; Dong et al. 2022; Frąc et al. 2021) or under air-moist conditions with varying relative humidity from 45 to 100% (e.g. Erol and François 2014; Viccaro 2018; Zhao et al. 2024). In contrast, Kim and Oh (2019) cured their samples at ambient conditions, drying them in the oven and re-saturating them by placing them in water for 2 to 5 days. Song et al. (2019) used a consistometer to cure the samples at elevated temperatures (60 °C) and pressure (20 MPa). Due to the ongoing hydration process, the time when the measurement is conducted after the manufacturing can become relevant. In the different studies, various hydration times were chosen ranging from measurement at 7 (Berktaş et al. 2020) to 30 days (Erol and François 2014). Some studies evaluated the influence of the hydration time on the thermal properties by measurement at different hydration times up to 30 days (Bentz 2007; Erol and François 2014; Park et al. 2011), finding that after the first days, no significant changes in the thermal parameters occurred.

To understand how different measurement methods and sample preparation methods can influence thermal properties, it is therefore essential to understand the material properties that influence thermal properties. Grouting samples are porous samples. Thus, the properties of the sample depend on the properties of the solid part (i.e. mineralogy, grain contact, arrangement) and of the pores (i.e. pore size, pore distribution, pore filling). As the enhancement of thermal conductivity is the main focus of most of the studies, the influence of additives is well-studied in the literature (e.g. Allan 1997; Erol and François 2014; Viccaro 2018). The most common additives are silica sand and graphite. While silica sand increases the thermal conductivity, it has a decreasing effect on the specific heat capacity of the grouting material (Allan 1997; Kim et al. 2017; Kim and Oh 2019). Although small amounts of graphite increase the thermal conductivity of the grout, it also can have a negative effect on the porosity and the workability of the material (Erol and François 2014; Pascual-Muñoz et al. 2018; Song et al. 2019; Viccaro 2018). The porosity of the grouting material is highly dependent on the water–solid ratio

(W/S), the ratio of water and the raw material used for manufacturing (Dong et al. 2022; Lafhaj et al. 2006; Stark and Wicht 2013). More importantly, the pore size distribution is also dependent on the W/S, which has a significant impact on the hydraulic conductivity of the system (Stark and Wicht 2013). Most material properties are negatively influenced by a high W/S. As the pore fluids have a lower thermal conductivity than the solid material, increasing W/S decreases the thermal conductivity of the grouting material (Allan 1997). Park et al. (2011) showed for their studied materials a decrease in the thermal conductivity by 0.01 to 0.07 W m⁻¹ K⁻¹ when increasing the W/S by 0.1. Air as a pore fluid has a significantly lower thermal conductivity than water. Hence, thermal conductivity increases with increasing saturation (Delaleux et al. 2012). At the same time, specific heat capacity increases with increasing water content (Kim et al. 2017; Kim and Oh 2019).

As highlighted before, in the literature on grouting materials, the main focus is on the determination and improvement of thermal conductivity. Most often, the volumetric heat capacity is neglected. Yet, there is no standard measurement procedure for the determination of the thermal properties of grouting materials. Hence, various laboratories worldwide have developed their own procedure. Rarely, comparisons between different measurement methods or different sample preparation procedures are conducted apart from the studies by Kim and Oh (2020) and Do et al. (2017).

Hence, the objective of this study is the comprehensive comparison of analysis methods to determine the thermal conductivity and the volumetric heat capacity of grouting materials for BHE. This study does not aim to develop a new procedure, instead it highlights the weaknesses and strengths of the different existing methods and provides recommendations for the analysis procedure based on the findings of this study. This is the first study that provides a comprehensive overview of the analysis methods for the thermal properties of grouting materials. For the first time, the influence of not only the measurement method, but also the sample preparation procedure on the determination of the thermal properties is thoroughly evaluated. In extensive laboratory experiments, different measurement methods are applied and sample preparation procedures are systematically varied and evaluated about the mixing speed, curing conditions and hydration time. An estimation procedure for volumetric heat capacity is also derived. Thereby, this study contributes to the consistency and comparability between studies on the thermal properties of grouting materials. The findings of this study help interpret the results of different studies with regard to the analysis methods. Furthermore, they offer a guideline to decide, which method should be applied to analyse the thermal properties of grouting materials, which therefore is a first step for a standardised approach.

Materials and methods

The general workflow of the analysis of grouting materials is presented in Fig. 1. Further information can be found in the respective chapters. The influencing parameters of the measurement method and the sample preparation on the analysis of thermal conductivity and volumetric heat capacity of grouting materials are systematically evaluated. As common for method development, first, the measurement method is optimised, representing a good controllable system. Afterwards, the sample preparation method is also evaluated. Thermal conductivity is analysed with two different transient measurement

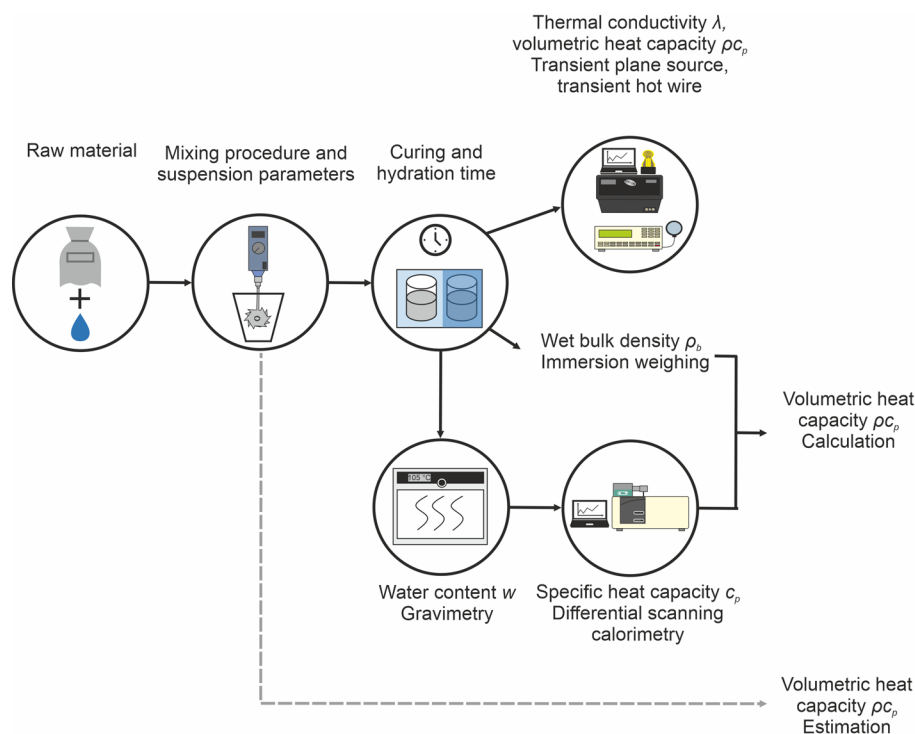


Fig. 1 Workflow for the determination of thermal conductivity λ and volumetric heat capacity ρc_p of grouting materials applying different methods

methods, which also determine volumetric heat capacity. The volumetric heat capacity results from these transient methods are compared to volumetric heat capacities calculated from DSC results. Finally, using the relationships between material properties, volumetric heat capacities are estimated from W/S and suspension properties.

Material

A range of commercially available materials is analysed. This includes seven different grouting materials from five manufacturers with varying material properties. The materials vary in their mineralogy and chemistry (main components, additives), the W/S, the suspension density and, therefore, their thermal properties. The variety of materials allows generalisations of outcomes of this study about grouting materials. Table 1 provides an overview of the materials and the investigation program applied to the different materials. A detailed list of the applied methods and the corresponding sample conditions can also be found in the supplementary information (Table A-4).

Sample preparation

The grouting samples are manufactured based on the specifications of the manufacturers. From a homogenised sample, the raw material is weighed for the manufacturing of a defined suspension volume of 2.5 L (balance accuracy 0.1 g). A defined mixing bucket (Carl Roth GmbH + Co. KG, volume 5 L, top diameter = 180 mm, bottom diameter = 160 mm, height = 270 mm) is filled with tap water according to the provided

Table 1 Overview of the analysed grouting materials (M1–M7), their properties and the applied investigation program

Properties	M1	M2	M3	M4	M5	M6	M7
Water–solid ratio W/S [–]	0.80	0.80	0.30	0.60	0.38	0.57	0.45
Suspension density ρ_{sus} [g cm ⁻³] ^a	1.48	1.55	1.94	1.6	1.9	1.7	1.80
Composition	Cement-based	Cement-based	Cement-based	Cement-based	Cement-based	Cement-based	Cement, bentonite, clay and stone powders
Thermally enhanced	No	Graphite	Quartz	No information	Additives, fine aggregates	Additives	Aggregates
Investigation program	M1	M2	M3	M4	M5	M6	M7
Measurement method	×	×	×	×	×	×	×
Mixing speed	×	×	×	–	×	–	–
Curing conditions	×	×	×	–	×	–	–
Hydration time	×	×	×	×	–	–	–
Variation of W/S	×	–	–	–	–	×	×

^a Manufacturer value

W/S. An overhead stirrer is used as a mixing device (IKA Eurostar 60 digital, dissolver stirrer R1300, diameter = 80 mm). The dissolver is positioned in a way that the vertical distance between the bottom of the vessel and the centre of the dissolver corresponds to the radius of the dissolver. The dissolver is aligned horizontally in the centre of the measuring beaker. The mixing speed is set to a defined rotation velocity (650 rpm and 2000 rpm, respectively). The grouting material is added evenly and quickly using a laboratory shovel. The suspension is stirred for 5 min.

The suspension properties are determined according to the following Chapter (**Suspension properties**). The suspension is filled in moulds with a defined geometry. For thermal conductivity measurements, the suspension is filled in cylinders (Plexiglass, 10 cm diameter, about 5 cm height), which are fixed to a planar polyvinyl chloride (PVC) plate, taking care of an even and smooth surface of the sample. For the other analyses, the suspension is filled in three separate silicon cubes (5 cm in length). The moulds are cured under defined conditions (at room temperature 20 ± 2 °C; under deionised water and air-moist $85 \pm 5\%$ relative humidity). Analyses of the hydrated samples are conducted at defined hydration times (from 7 up to 365 days).

Suspension properties

Suspension properties are analysed based on the recommendations of the Association of German Engineers VDI 4640-2 (Verein Deutscher Ingenieure 2019). Suspension stability is determined for the time of 3 h in a cylinder (volume 250 mL). The suspension

density ρ_{sus} [g cm^{-3}] is analysed with a mud balance. The workability is analysed with the Marsh funnel based on German Industrial Standard DIN 4127 (Deutsche Norm 2014).

Wet bulk density, water content, porosity and saturation

Wet bulk density ρ_b [g cm^{-3}] is analysed using immersion weighing according to German Industrial Standard DIN 17892-2 (Deutsche Norm 2015). Water content w [–] is determined by oven drying (at 105 °C) based on German Industrial Standard DIN EN ISO 17892-1 (Deutsche Norm 2022). From dried and ground samples, solid density ρ_s [g cm^{-3}] is analysed with the pycnometer method according to German Industrial Standard DIN ISO 17892-3 (Deutsche Norm 2016b). Applying the following Eqs. (1) to (3), dry bulk density ρ_d [g cm^{-3}], porosity ϕ [–] and saturation S_r [–] are calculated (Prinz and Strauß 2018):

$$\rho_d = \frac{\rho_b}{1 + w} \quad (1)$$

$$\phi = 1 - (\rho_d / \rho_s) \quad (2)$$

$$S_r = \frac{\phi_w}{\phi} = \frac{w(\rho_d / \rho_w)}{\phi} \quad (3)$$

ϕ_w [–] is the water-filled pore space and ρ_w [g cm^{-3}] is the density of water.

Thermal conductivity measurement

The thermal conductivity of the hydrated samples is measured with two different measurement methods: (1) transient hotwire (THW) method and (2) transient plane source (TPS) method. Thermal conductivity is measured by evaluating the temperature response due to a defined heat load. Both methods applied in this study use a transient measurement principle. The THW method using needle probes is based on the standard ASTM D5334-22a (ASTM International 2023). The heat load is applied to the sample using an electrical resistor. The temperature is recorded with time directly at the heat source. Under the assumption of an infinite medium, the temperature increase is evaluated based on the infinite line source method. The method is modified for surface probes under the assumption that the heat propagates in half-space direction through the specimen. The THW method is applied using a stiff, half-space surface probe (ISOMET 2104, Applied Precision Ltd., Slovakia) that is placed on the surface of the sample. The measurement probe is calibrated for thermal conductivities from 0.3 to 3.0 $\text{W m}^{-1} \text{K}^{-1}$. Two cylindrical samples are separately analysed and the mean value is calculated.

The TPS method is described in Gustafsson (1991) and in German Industrial Standard DIN EN ISO 22007-1 (Deutsche Norm 2021a; b) in detail. The measurement probe is shaped in form of a nickel-metal double spiral. The user-defined heat load is induced by applying an electrical voltage. The temperature response of the sample is derived from the change of electrical resistance. Evaluation of the temperature increase is based on the solution of the heat transport equation under the assumption of a defined number of concentric ring heat sources. The TPS method is applied with a full space probe (HotDisk TPS1500, C3 Prozess- und Analysentechnik, Germany)

by placing a flexible probe between two sample cylinders of the same material. For the TPS method, the data acquisition is conducted with the software *Hot Disk Thermal Constants Analyser* (Version 7.4.17). The software enables control of the quality of the measurements by direct interpretation of the raw data and model fit.

The samples are measured at room temperature (20 ± 2 °C) and original water content. Thermal conductivity measurements with the THW are carried out at the conditions the samples were cured at, i.e. under water or air-moist. The measurements are carried out in a closed, thermally insulated container that is protected from sunlight. The samples are conditioned to the respective temperature before measurement. In between repeated measurements, the samples are always stored at the cured conditions. The same specimens are used for both, THW and TPS, measurements to enable valid comparison of the methods.

Specific heat capacity

Calorimetry is used to determine the amount of heat that must be applied or is generated during a physical or chemical transformation of a material, which results in a change of the internal energy of the material, referred to as the enthalpy H at constant pressure (Haines 2002). Differential scanning calorimetry is based on the difference of the heat flow between a material and a reference sample as a function of temperature. The heat flows are derived from the continuously measured temperatures of the material and the reference. By integrating the peak area of the difference signal, the change in enthalpy is calculated. One frequently applied reference material is sapphire. Further information on the measurement principle can be found e.g. in Höhne et al. (2003).

In this study, the specific heat capacity of the grouting materials is measured with a differential scanning calorimeter (DSC, No. 204 F1 Phönix, Netzsch, Germany) applying the sapphire comparison method according to German Industrial Standard DIN EN ISO 11357-4 (Deutsche Norm 2021a; b). The DSC is equipped with a cooling unit (Intra-Cooler IC85, Netzsch, Germany). For samples containing water, the enthalpy peaks of the water would superimpose the specific heat capacity signal of the grout. Thus, DSC measurements are conducted on ground, dried samples (oven dried at 105 °C). The material is weighed into crucibles (aluminium, 40 μ L, Netzsch) using a microfine balance (Cubis II MCE 125P, accuracy ± 0.01 mg). The measurements are carried out in a nitrogen atmosphere (flow rate: 20 mL h⁻¹). The temperature range is -16 °C to 45 °C with a heating rate of 10 K min⁻¹. Data acquisition and analysis are performed using associated *Proteus*[®] software. The specific heat capacity is an additive quantity (Bentz 2007). Thus, the specific heat capacity at original water content $c_{p,f}$ [kJ kg⁻¹ K⁻¹] is the weighted arithmetic mean of the specific heat capacities of the components:

$$c_{p,f} = \frac{w}{1+w} c_{p,w} + \left(1 - \frac{w}{1+w}\right) c_{p,d} \quad (4)$$

$c_{p,d}$ [kJ kg⁻¹ K⁻¹] is the specific heat capacity of the dried sample. The specific heat capacity of water $c_{p,w}$ [kJ kg⁻¹ K⁻¹] is determined beforehand in the investigated temperature range and compared to literature data.

Volumetric heat capacity

The volumetric heat capacity is analysed with three different methods. It is (1) calculated from DSC measurements for dried and saturated samples ($\rho c_{p,d}$ and $\rho c_{p,f}$ [MJ kg⁻¹ K⁻¹]), respectively:

$$\rho c_{p,d} = \rho_d \times c_{p,d} \quad (5)$$

$$\rho c_{p,f} = \rho_b \times c_{p,f} \quad (6)$$

In addition, measurements of the volumetric heat capacity of the samples at the original water content are conducted during the measurement of thermal conductivity with (2) the THW as well as with (3) the TPS (Chapter **Thermal conductivity measurement**). The THW method uses the temperature change with time to derive the thermal diffusivity α . Applying the TPS method, thermal diffusivity is derived through parameter fit. Volumetric heat capacity is calculated applying:

$$\rho c_p = \frac{\lambda}{\alpha} \quad (7)$$

Measurement uncertainties

Measurement uncertainties of the analysed properties are calculated based on the *Guide to the Expression of Uncertainty in Measurement* (ISO IEC 98-3 2008). For repetitive measurements, the standard deviation s is determined according to the following equation:

$$s = \sqrt{\frac{1}{n-1} \sum_{i=1}^n (x_i - \bar{x})^2} \quad (8)$$

n is the number of measurements, x_i is the measurement value and \bar{x} is the arithmetic mean of all measurement values. With the Student's t -distribution, the standard uncertainty u_s with a confidence interval of 0.68 is calculated.

$$u_s = t \frac{s}{\sqrt{n}} \quad (9)$$

Combined measurement uncertainties are calculated from the propagation of uncertainties. In the supporting information (Table A-5), the measurement uncertainties for the different parameters are summarised.

Results and discussion

First, the measurement methods for the determination of thermal conductivity and volumetric heat capacity are evaluated. Then, the sample preparation is evaluated regarding (1) mixing speed, (2) curing conditions and (3) hydration time. In the third step, the influence of the W/S on the thermal properties is discussed. The results of

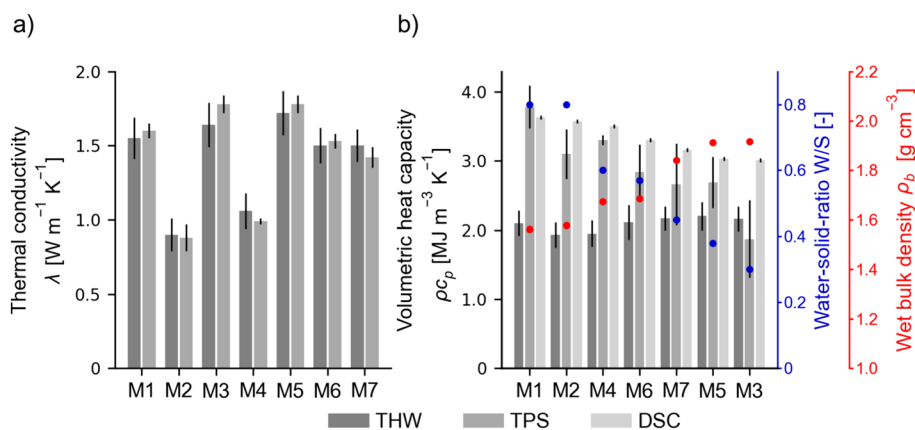


Fig. 2 Comparison of measurement methods for the analysis of **a** thermal conductivity and **b** volumetric heat capacity. The black lines indicate standard uncertainties (Chapter **Measurement uncertainties**). Samples preparation: Mixed at 2000 rpm, cured under water, hydration time 28 days and measured at 20 °C

this study are additionally used to derive an estimation procedure of the volumetric heat capacity from the W/S and the suspension density ρ_{sus} .

Measurement method

Thermal conductivity

The thermal conductivities of the analysed samples range from 0.9 to 1.8 $\text{W m}^{-1} \text{K}^{-1}$. Figure 2a shows the thermal conductivity results of the different measurement methods.

The thermal conductivity is measured with two transient measurement methods, the transient hotwire (THW) and the transient plane source (TPS) method. Both methods lead to comparable results. The mean deviation between both methods is only 4.5%. The maximum deviation is 8% for the material M3, and thereby still below the 10% measurement uncertainty stated by the manufacturer.

The accuracy of the thermal conductivity measurement is highly influenced by the quality of the thermal contact between the measurement probe and the sample or sample surface. The manufacture of the sample with a smooth and plane surface is crucial. The measurement probes of the THW and the TPS have different specifications. The THW probe is more stiff, which is accounted for by the manufacturer of the device during the calibration of the probe. The TPS probe is more flexible, which can partly compensate irregularities in the sample surface. The results show that both methods are suitable for the measurement of thermal conductivities of grouting materials. It should be noted that the recommendations on the measurement method of thermal properties refer especially to grouting materials. The thermal conductivity measurement with surface probes (THW, TPS) is recommended for solid samples with smooth surfaces, such as grouting materials or rocks, as surface probes ensure a good thermal contact. Regarding the measurement of unconsolidated material, such as soils and sands, a needle probe can be the better choice. However, this comparison is not considered in this study. Concerning validation of the results, measuring with two measurement methods is recommended when available and feasible. However, for the sake of clarity, further results for thermal conductivity are presented for TPS measurements only.

Volumetric heat capacity

The determined values for the volumetric heat capacity of the grouting samples at saturated conditions range from 1.9 to 3.8 MJ m⁻³ K⁻¹ (Fig. 2b). The deviation between the different measurement methods is rather high. For nearly all materials, the lowest values are measured with the THW and the highest values are determined with the DSC. On average, the volumetric heat capacity measured with the THW is 36% below that of the DSC, and the volumetric heat capacity measured with TPS is 13% below that of the DSC. Values are compared at room temperature. With the DSC, specific heat capacities are always analysed above a temperature range. In the supplementary information (Fig. A-1), the specific heat capacities are complementary shown for the entire analysed temperature range (– 10 to 40 °C) with only a minor increase in the specific heat capacities to a maximum of 0.05 kJ kg⁻¹ K⁻¹ in the range of 5 to 40 °C. Investigating the plausibility of the measured volumetric heat capacities for the different materials, higher volumetric heat capacities should be evaluated for materials with higher W/S. The volumetric heat capacity of water predominately influences the volumetric heat capacity of the water-saturated grouting material (Table 1, Eq. 6). The values derived with the THW method show no correlation between higher W/S and higher volumetric heat capacities. By comparing the values for M2 and M3, the materials with the highest and lowest W/S, respectively, even higher values are measured for the material M3 with the lower W/S. The TPS results are more consistent, however not for all samples. By comparing the values of M7 and M5 (W/S=0.45 and 0.38), the volumetric heat capacity of M7 is lower than that of M5. Only the DSC values are plausible considering the relationship between the density and the composition of the sample (W/S). A detailed discussion on the relationship between the W/S and the properties of the grouting materials (water content, density, specific heat capacity) is included in Chapter **Influence of the water-solid ratio (W/S)**.

The standard uncertainties are also rather high for the transient measurement methods and the repeatability is low as indicated by the error bars (Fig. 2b). Average relative uncertainties for the THW and the TPS are 9% and 15%, respectively. In contrast, the standard uncertainty of the volumetric heat capacity determination with DSC is only ±0.03 MJ kg⁻¹ K⁻¹, which accounts for a relative error of 1%.

The high variation of volumetric heat capacity between the three measurement methods can be explained with the difference in the measurement methods. The samples for the transient methods (THW, TPS) are measured at the original water content and as a bulk. The measurement probes are placed at the surface of the sample and only a specific sample volume is analysed. Thus, inhomogeneity, surface and structure effects add to the uncertainty of the measurement. In contrast, the samples for measurement with the DSC are dried and ground resulting in very homogeneous samples. Repeated measurements on different aliquots prove the repeatability of the measurements. Volumetric heat capacity as a composite parameter is calculated with the water content and the bulk density determined on bulk samples. Hence, uncertainties increase due to the necessity of conducting three different analyses.

In addition, determination of the volumetric heat capacity from the transient measurements is based on curve fitting of the temperature change due to a defined heat input (Chapter **Thermal conductivity measurement**). Hence, the fit is based on model assumptions. Furthermore, contact thermal resistance can influence the results of the

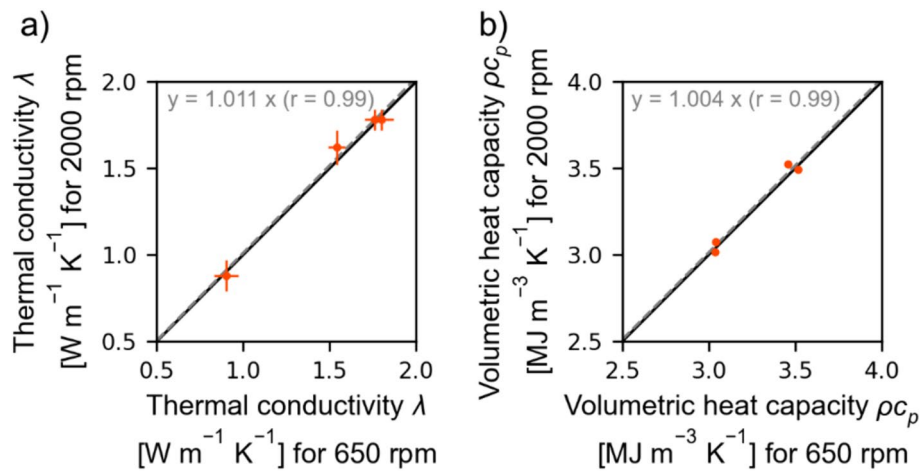


Fig. 3 Comparison of **a** thermal conductivities and **b** volumetric heat capacities with varying mixing speed. Sample preparation: cured under water, hydration time 28 days and measured at room temperature (20 °C)

fit. As natural samples typically have rougher surfaces compared to ideal flat surfaces, there is always a higher error due to the irregular contact between the probe and the sample surface. DSC, on the other hand, is a very accurate method to measure the specific heat capacity of dry grouting materials, rocks or unconsolidated materials as the specific heat capacity is directly derived from the heat flow. In conclusion, measuring the volumetric heat capacity with transient measurement methods, such as THW and TPS, can only provide first and rough estimates with high uncertainty. Hence, the DSC is our recommended method for the determination of the volumetric heat capacity of grouting materials. Accordingly, further results for the specific heat capacity and volumetric heat capacity, respectively, are only presented for the DSC method.

Sample preparation

The sample preparation is crucial for the quality of an analysis. Following, the influence of the sample preparation on the thermal conductivity and volumetric heat capacity is evaluated.

Mixing speed

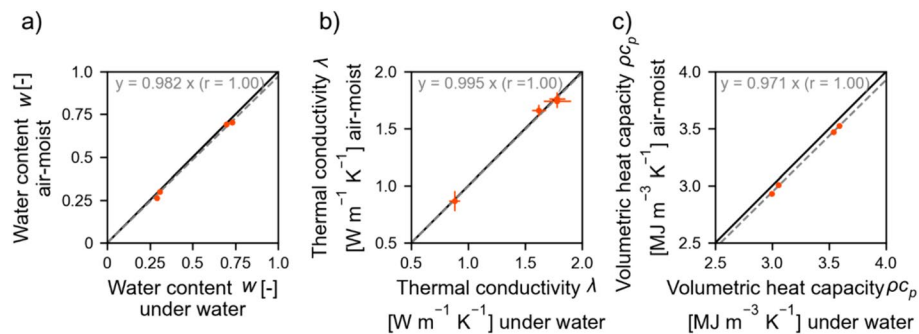
The mixing procedure of the grouting material is essential to ensure a good blend of the raw material and the mixing water and, therefore, manufacture a homogeneous material. In this study, two different mixing velocities (650 and 2000 rpm) and their effect on the thermal properties are compared (Fig. 3).

The results of the studied materials show almost no measurable influence of the mixing speed on the thermal conductivity and the volumetric heat capacity. This applies to grouting materials with high W/S (M1, M2) as well as to grouting materials with low W/S (M3). However, the mixing speed influences the suspension parameters and the structure of the sample (Table 2).

The suspensions mixed at lower mixing speed indicate inhomogeneity and the formation of lumps. Furthermore, they show a quality loss in the flow parameters. For example, material M2 has a higher suspension stability at a lower mixing speed. Significantly

Table 2 Suspension properties and porosity of the grouting materials at varying mixing speed (650 rpm and 2000 rpm)

Sample	M1		M2		M3		M5	
	650	2000	650	2000	650	2000	650	2000
Suspension stability [%]	0.8	0.8	1.6	0.8	0.4	0.4	1.6	1.6
Workability (1 L) [s]	43	48	42	62	68	94	93	181
Suspension density ρ_{sus} [g cm ⁻³]	1.53	1.54	1.54	1.55	1.93	1.92	1.85	1.87
Porosity φ [%]	65.1	63.9	65.5	64.9	44.2	43.3	46.2	45.4

**Fig. 4** Comparison of **a** water contents, **b** thermal conductivities and **c** volumetric heat capacities for varying curing conditions. Sample preparation: mixed at 2000 rpm, hydration time 28 days and measured at room temperature (20 °C)

lower Marsh funnel flow times (15–50%) are observed for the materials M2, M3 and M5. The porosity of all materials increases slightly for mixing at 650 rpm compared to 2000 rpm. Thus, between the two mixing speeds a clear recommendation for 2000 rpm can be made. However, the influence of the mixing method on the properties of cementitious material is complex (e.g. Dils et al. 2012). It depends not only on the mixing speed but also on the type of mixer and the mixing procedure, including, for example, the amount of material and the mixing time. Hence, the recommended mixing speed is not transferable to other mixing devices. However, it is highlighted to always use a mixing speed that ensures a homogeneous mixture during the manufacturing of grouting materials.

Curing conditions

To analyse the influence of the curing conditions during hydration, the grouting samples are cured under two different conditions: submerged under water and air-moist (85 ± 5% relative humidity) conditions (Fig. 4).

Curing conditions are expected to influence the water content due to evaporation processes. Figure 4a shows slightly lower water content under air-moist curing for all samples. On average, the water content is 4% lower for air-moist cured grouting samples, with a maximum of 9% for material M3. Thus, the total saturation of $S_r = 1.0$ as achieved with the samples cured under water is not always achieved. A decrease in thermal conductivities due to the lower water content is not measured (Fig. 4). This could be explained by the evaporation process. Water evaporates from the sample

at the surface, resulting in an inhomogeneous water distribution inside the grouting sample. Thus, the major part of the grouting sample is not affected by the curing conditions during the observed hydration time of 28 days. Figure 4a shows that the decrease in water content due to evaporation is minor, which is related to a low water vapour pressure at a relative humidity (RH) of about 85%. However, Do et al. (2017) showed a decrease in thermal conductivities, when storing samples under air-moist conditions instead of under water. Do et al. (2017) compared the curing under water, the curing in a wet chamber at 100% RH and a wet chamber at 50% RH. For controlled low strength materials (CLSM) with cementless binders, they evaluated a decrease in thermal conductivities of > 50% at 50% RH and about 36% at 100% RH.

The specific heat capacity of dry samples is not affected by the curing conditions. However, since the water content is used for the calculation of volumetric heat capacity at original water content (Eq. (4), lower water contents result in lower volumetric heat capacities (Fig. 4c). For material M1, the values are lower by $0.04 \text{ MJ m}^{-3} \text{ K}^{-1}$, for M2, the values are lower by $0.02 \text{ MJ m}^{-3} \text{ K}^{-1}$. For material M3, the values are lower by $0.05 \text{ MJ m}^{-3} \text{ K}^{-1}$. The influence of the curing conditions could also be shown by Bentz (2007) who evaluated higher specific heat capacity for samples cured under water than cured under air-moist conditions. From the results, under-water curing of the grouting samples can be recommended as in this way complete saturation of the samples can be achieved. Furthermore, easily controllable curing conditions can be maintained. Carbonation reactions with the CO_2 of the air can change the composition of the material surface (Verein Deutscher Zementwerke e.V. 2002). Thus, by curing the sample under water, carbonation processes at the surface of the samples can be hindered. However, the curing in deionised water can cause leaching of the sample.

Hydration time

The hydration of cementitious material is a continuous process (e.g. Aïtcin 2016; Bullard et al. 2011). Thus, the age of the grouting samples has to be considered for the analyses of thermal properties. Hence, thermal conductivity and specific heat capacity are measured dependent on the hydration time (Fig. 5). The samples are cured under water and measured at specific measurement days up to a hydration time of a year, to gain representative measurement values for the long-time development. Since the volumetric heat capacity of water-saturated samples is calculated with the wet bulk density and the water content, Fig. 5c and d complementary show these values about the hydration time. Volumetric heat capacity is not shown, as wet bulk density is not evaluated for the entire hydration time.

(See figure on next page.)

Fig. 5 Thermal conductivity (a), specific heat capacity (b), wet bulk density (c) and water content (d) with increasing hydration times. Measurement uncertainties of the specific heat capacity below $0.01 \text{ kJ kg}^{-1} \text{ K}^{-1}$ are not shown. Values from single measurements are marked as open circles. The dashed line represents the reference value at 28 days. Sample preparation: mixed at 2000 rpm, cured under water and measured at room temperature (20 °C)

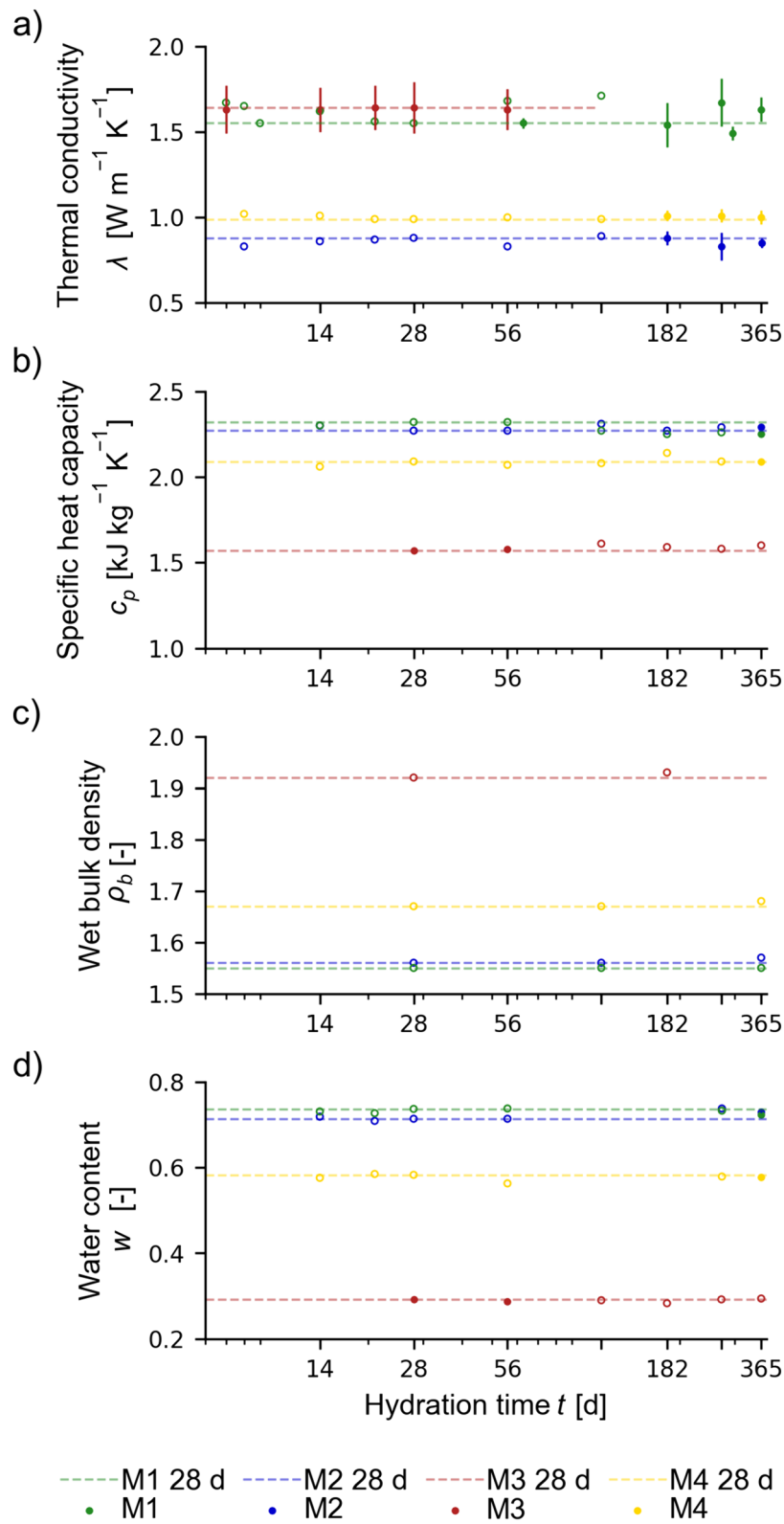


Fig. 5 (See legend on previous page.)

Regardless of the material composition, from 7 and 14 days, respectively, no significant influence of the hydration time on the thermal conductivity and the specific heat capacity is observed. The variations of the values lie within the range of the measurement error. Changes caused by the ongoing hydration process cannot be resolved by the measurements. By comparing the specific heat capacities (Fig. 5b) and the water contents (Fig. 5c), higher values in the water content directly result in higher values of the specific heat capacity, e.g. for material M4 at 182 days. The wet bulk density of the samples shows little change during the analysed hydration time, indicating that the volumetric heat capacity does not change with later hydration times as well.

The results of this study follow the findings of other studies conducted about thermal conductivity (Bentz 2007). Most reaction processes, where free water is chemically bound into silicate hydrate phases, take place within the first hours and days (Stark and Wicht 2013). From there on, only marginal changes in the chemistry of the materials are expected. Regarding the specific heat capacity of concrete, Schutter and Taerwe (1995) studied the early hydration stage (1–7 days). They showed a decrease in the specific heat capacity with an increasing degree of hydration in the order of magnitude of about 13%. Comparable results with cement paste were obtained by Bentz (2007). They showed that during the early hydration stage (<7 days), the specific heat capacity decreased significantly before it reached an almost constant value. Measurement of the samples <7 days is therefore not conducted during this study. At earlier time data, the strength of the sample is low. Handling of the sample is difficult. To maintain the integrity of the sample, only >7 days' measurements are conducted. However, for shallow geothermal energy systems, the comparison of this study aims to identify a value that is representative of the material during the application ($\gg 7$ days). In some standards, the measurement of material properties at 28 days of hydration time is stated (Deutsche Norm 2016a; Verein Deutscher Ingenieure 2019). Figure 5 highlights that this value can be used representatively for more mature samples.

Influence of the water–solid ratio (W/S)

The W/S of the studied materials ranges from 0.3 to 0.8. Furthermore, variation ($\pm 5\%$ and $\pm 10\%$) of the water content of the value recommended by the manufacturer is analysed for materials M1 (W/S=0.8), M6 (W/S=0.57) and M7 (W/S=0.45) to extend the data. Figure 6 shows how the water content, wet bulk density and porosity as well as the thermal properties of saturated samples depend on the W/S.

The calculated correlations are based on values from varying grouting materials. Regarding this, the correlations do not represent definite physical or chemical relationships, however, highlight to what extent the W/S influences the properties of the grouting materials. There is a clear linear relationship between the W/S and the corresponding water content for the materials analysed in this study (Fig. 6a). The W/S is the ratio of the water mixed with the raw grouting material (powder). During the hydration of a cement, free water is chemically bound into silicate hydrate phases (Schutter and Taerwe 1995; Stark and Wicht 2013). Thus, water in hardened cement can be present as free water, physically bound water or chemically bound water. Experimentally, it cannot easily be distinguished between the three different types of water. However, the evaporable water, as determined with the water content, includes mainly the free water, the

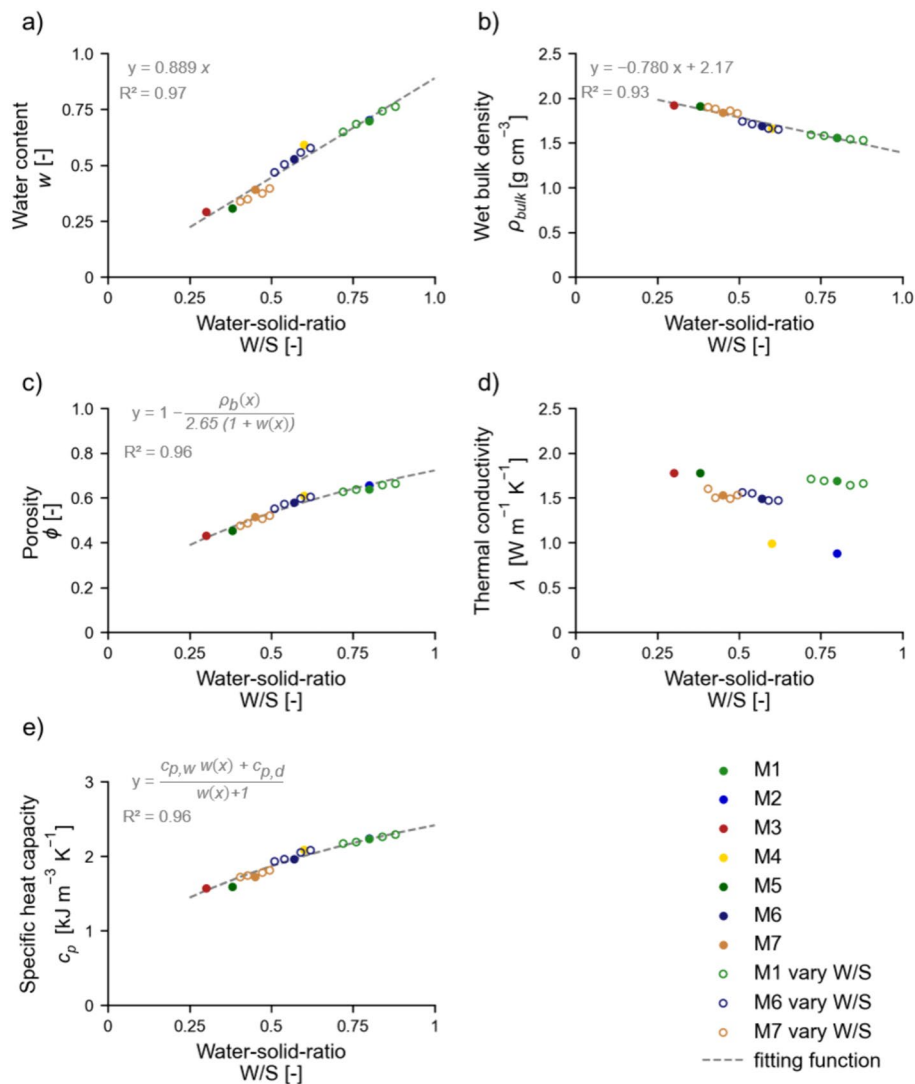


Fig. 6 Influence of the water–solid ratio on **a** water content, **b** wet bulk density, **c** porosity, **d** thermal conductivity and **e** specific heat capacity. Sample preparation: mixed at 2000 rpm, cured under water, hydration time 28 days and measured at room temperature (20 °C). Including additional values varying the W/S for materials M1, M6 and M7 to increase the database. Fitting functions for c) and e) based on Eqs. 4 and 6

physically bound water and part of the chemically bound water (Adam 2006). In a closed system (curing under water), the amount of water cannot be reduced. Thus, the decrease of the water content as compared to the W/S describes the amount of water that is no longer accessible as evaporable water. The amount of chemically bound water depends mainly on the cement content, the clay content and other additives (e.g. plasticisers, liq-uifiers) of the raw material. Following the relationship between W/S and the water content, Fig. 6a shows with a degree of determination of 0.97 that about 10% of the added water is bound chemically for the analysed materials.

There is a nearly linear relation between the W/S and the wet bulk density (Fig. 6b) for the analysed W/S range of 0.3 to 0.8. Higher W/S result in lower densities. The varying amounts of different additives (e.g. quartz, graphite) are leading to deviations from the

linear correlation. Accordingly, higher W/S result in higher porosities (Fig. 6c). Porosities are analysed in the range of 0.43 to 0.66. With higher porosities, lower thermal conductivities are expected. However, Fig. 6d shows that between the W/S and the thermal conductivities measured in this study, no general relationship can be established.

The thermal conductivities of the analysed samples range from 0.9 to 1.8 W m⁻¹ K⁻¹. The grouting materials have varying amounts of different additives (e.g. silica sand, graphite). This effect superimposes the effect of the W/S. However, for the same material at varying W/S, lower thermal conductivities with higher W/S are evaluated. In contrast, the specific heat capacities of saturated samples show a strong dependence on the W/S (Fig. 6d). This relation is not surprising, as the specific heat capacity of a composite is the weighted arithmetic mean of the specific heat capacity of the components [Eq. (4)]. The specific heat capacities of the dry samples (at 20 °C) show only minor variations between 0.76 to 0.92 kJ kg⁻¹ K⁻¹, with an average value of 0.83 kJ kg⁻¹ K⁻¹. The specific heat capacity of water is higher than that of one of the mineral components ($c_{p,w} = 4.18$ kJ kg⁻¹ K⁻¹ at 20 °C). Hence, the specific heat capacities of the saturated samples mainly depend on the water content, which also depends on the porosity. Higher specific heat capacity of water-saturated samples with higher W/S was also shown by other studies (Bentz 2007; Kim and Oh 2019; Marshall 1972). Concerning the volumetric heat capacity, the decreasing effect of the W/S on the wet bulk density and the increasing effect of the W/S on the specific heat capacity of the saturated samples superimpose each other. However, the increasing effect of the specific heat capacity of the water is stronger than the decreasing effect of the density.

Estimation of the volumetric heat capacity

The W/S values as analysed in this study range from 0.3 to 0.8, which is common for commercially available grouting materials in Germany. Here, an estimation of the volumetric heat capacity of saturated grouting materials is proposed.

Based on the results of this study, the following assumptions are made:

- (1) The specific heat capacities of dried grouting materials can be estimated with an average value of 0.83 ± 0.05 kJ kg⁻¹ K⁻¹ at 20 °C based on the measurements of the specific heat capacity of the grouting materials in this study.
- (2) An empirical relationship between the W/S and the water content of grouting materials can be determined (Fig. 6a).
- (3) The wet bulk density can be estimated with the suspension density. Figure 7 shows, that wet bulk density is close to the density of the suspension. The maximum difference for the evaluated materials is only 2.7%, which is expected in a closed system like the laboratory. Apparently, diffusion and exchange processes occur only to an insignificant extent.

With these assumptions, a relationship is derived to estimate the volumetric heat capacity of grouting materials that can be applied only with the information available at a construction site, namely the measured suspension density and the W/S given by the manufacturer. The following equation summarises the calculation of the estimated volumetric heat capacity $\rho c_{p,est}$ [MJ kg⁻¹ K⁻¹] at 20 °C:

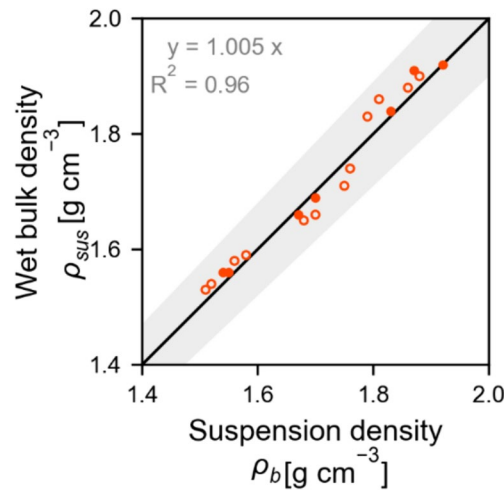


Fig. 7 Correlation between the wet bulk density of the hydrated grouting samples and the suspension density. Sample preparation: mixed at 2000 rpm, cured under water, hydration time 28 days. Including additional values varying the W/S for materials M1, M6 and M7 to increase the database (open circles). The shaded area represents an error range of $\pm 5\%$

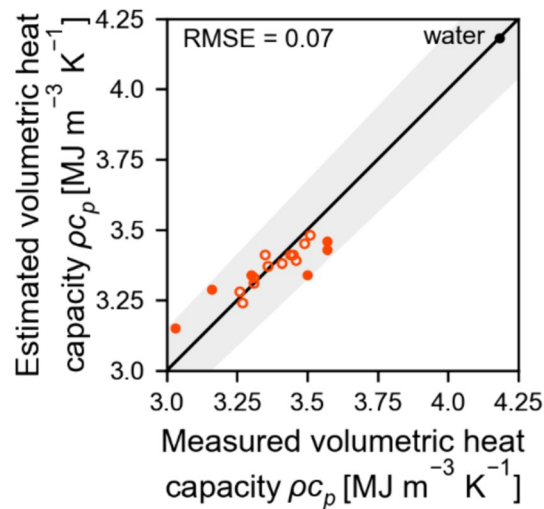


Fig. 8 Comparison of the measured and the estimated volumetric heat capacities ρ_{c_p} . Sample preparation: mixed at 2000 rpm, cured under water, hydration time 28 days, measured at room temperature (20 °C). Including additional values varying the W/S for materials M1, M6 and M7 to increase the database (open circles). The shaded area represents the error range of $\pm 5\%$

$$\begin{aligned} \rho_{c_{p,est}} &= \rho_{sus} (C \times W/S \times c_{p,w} + (1 - C \times W/S) \times c_{p,d}) \\ &= \rho_{sus} (0.89W/S \times 4.18MJm^{-3}K^{-1} + 0.11W/S \times 0.83MJm^{-3}K^{-1}) \end{aligned} \quad (10)$$

The coefficient C is empirically derived from the correlation between W/S and the water content (Fig. 6a). Figure 8 demonstrates that a feasible estimate can be obtained.

All estimated values are in the error range of $\pm 5\%$. The average difference between estimate and measurement value is only 1.7%. Thus, the estimated values are more accurate than values analysed with THW and TPS methods, which have a

measurement accuracy of about 5–10%. Deviations can be explained by the composition of the materials and by the uncertainty of the combined measurement value of the volumetric heat capacity, which is calculated from three independent measurements. For planners of shallow geothermal energy systems, this estimation can provide valuable information. However, for this estimation, the mineralogical and chemical composition of the grouting sample is assumed to have a negligible influence compared to the W/S. This can result in a higher uncertainty of the estimate for materials with significantly different compositions. In addition, it has to be emphasised that this relationship is only valid for the comparisons conducted in this laboratory study. Further information on the behaviour and the properties of grouting materials at field conditions is therefore needed to validate our assumptions also for field sites.

Conclusion

In this study, analytical procedures for the determination of the thermal properties of grouting materials are evaluated. The influence of the measurement method and the sample preparation procedure on thermal conductivity and volumetric heat capacity is comprehensively investigated. Seven different grouting materials with varying water–solid ratios (W/S) and compositions are analysed. From the results of this study, we conclude the following:

- (1) Several evaluated factors have only a minor influence on determining the thermal properties, such as mixing speed, curing conditions, and hydration time. Furthermore, the transient methods applied to measure thermal conductivity provide consistent results.
- (2) The results indicate that thermal conductivity values from different studies using various analysis procedures are quite comparable.
- (3) For determining the volumetric heat capacity, the measurement method is shown to have a major influence on the results. The DSC method is the most precise method with measurement uncertainties of $\leq 1\%$. An alternative estimation procedure based on the relation between W/S, water content and volumetric heat capacity achieved better estimation of the volumetric heat capacity of the grouting materials than measurement with the transient methods ($< \pm 5\%$). Hence, the results from the transient methods should be used with caution regarding grouting materials.

Based on our findings, recommendations for standardised analysis of thermal conductivity and volumetric heat capacity of grouting materials are made:

- (1) Mixing of the raw material at a high mixing speed (for the dissolver used in this study 2000 rpm).
- (2) Curing the samples under water for 28 days at room temperature.
- (3) Measuring thermal conductivity with transient measurement methods using surface probes at the original sample condition.

- (4) Analysing the water content and wet bulk density. Using dried, ground samples for measurement of the specific heat capacity with differential scanning calorimetry (DSC). Subsequently, calculating the volumetric heat capacity.

In addition, an estimation procedure of volumetric heat capacity is introduced that can be applied with the information available at a construction site. The estimation is based on the data of this study including materials with varying compositions and W/S. The verification of the estimation method with other materials is planned.

Future studies should focus on the validation of the developed methods in this study. A comparison of laboratory results and field studies is therefore necessary to investigate the suitability of the proposed laboratory methods for determining effective in situ thermal properties of grouting materials. The analysis of grouting samples at saturated conditions represents an optimal case for the grouting material. In the field, the saturation however can vary from this assumption due to grouting in the vadose zone under seasonal changes and varying heat loads of the shallow geothermal system.

Abbreviations

BHE	Borehole heat exchanger
CLSM	Controlled low strength material
DIN	Deutsches Institut für Normung (German Institute for Standardisation)
DSC	Differential scanning calorimetry
GSHP	Ground source heat pump
PVC	Polyvinyl chloride
RH	Relative humidity
RMSE	Root mean square error
THW	Transient hot wire
TPS	Transient plane source
W/S	Water–solid ratio
VDI	Verein Deutscher Ingenieure (Association of German Engineers)

Latin and Greek symbols

α	Thermal diffusivity [$\text{m}^2 \text{s}^{-1}$]
C	Empirically derived coefficient
c_p	Specific heat capacity [$\text{kJ kg}^{-1} \text{K}^{-1}$]
$c_{p,d}$	Specific heat capacity of the dry sample [$\text{kJ kg}^{-1} \text{K}^{-1}$]
$c_{p,f}$	Specific heat capacity of the humid sample [$\text{kJ kg}^{-1} \text{K}^{-1}$]
$c_{p,w}$	Specific heat capacity of water [$\text{kJ kg}^{-1} \text{K}^{-1}$]
d	Day(s)
λ	Thermal conductivity [$\text{W m}^{-1} \text{K}^{-1}$]
n	Number of measurements
ϕ	Porosity [–]
ϕ_w	Water-filled pore space [–]
ρ_b	Wet bulk density [g cm^{-3}]
ρ_d	Dry bulk density [g cm^{-3}]
ρ_s	Solid density [g cm^{-3}]
ρ_{sus}	Suspension density [g cm^{-3}]
ρ_w	Density of water [g cm^{-3}]
$\rho_{c,p}$	Volumetric heat capacity [$\text{MJ m}^{-3} \text{K}^{-1}$]
$\rho_{c,p,d}$	Volumetric heat capacity of the dry sample [$\text{MJ m}^{-3} \text{K}^{-1}$]
$\rho_{c,p,f}$	Volumetric heat capacity of the wet sample [$\text{MJ m}^{-3} \text{K}^{-1}$]
r	Pearson coefficient
R^2	Degree of determination
s	Standard deviation
S_r	Saturation [–]
T	Temperature [$^{\circ}\text{C}$]
t	Time [s]
u_s	Standard uncertainty
w	Water content [–] or [%]
x_j	Measurement value
\bar{x}	Arithmetic mean of all measurement values

Supplementary Information

The online version contains supplementary material available at <https://doi.org/10.1186/s40517-024-00316-3>.

Supplementary Material 1

Acknowledgements

The authors would like to thank Madeline Dantin, Lucas Homann and Felix Voss for their help with the laboratory experiments. The authors would also like to thank the manufacturers for providing the grouting material. The helpful comments of the two reviewers are also gratefully acknowledged.

Author contributions

Methodology and study design: AA, PH and HS; laboratory analyses and data evaluation: AA, PH; visualisation: AA; funding acquisition: RZ, HS; supervision: PB; manuscript—first draft: AA; all authors read and approved the final manuscript.

Funding

Open Access funding enabled and organized by Projekt DEAL. This study was carried out within the framework of the joint project QEWS+, which is funded by the Federal Ministry for Economic Affairs and Climate, Germany (grant number: 03EE4020B, 03EE4020E).

Availability of data and materials

The datasets used and/or analysed during the current study are available from the corresponding author upon reasonable request.

Declarations

Competing interests

The authors declare that they have no competing interests.

Received: 12 March 2024 Accepted: 5 September 2024

Published online: 28 September 2024

References

- Aïtcin P-C. Portland cement. In: Aïtcin P-C, Flatt RJ, editors. *Science and technology of concrete admixtures*. Amsterdam: Elsevier; 2016. p. 27–51.
- Allan M. Thermal conductivity of cementitious grouts for geothermal heat pumps, FY Progress Report. BNL 65129. New York: Brookhaven National Laboratory. 1997.
- Allan M, Kavanaugh S. Thermal conductivity of cementitious grouts and impact on heat exchanger length design for ground source heat pumps. *HVAC&R Res*. 1999;5:85–96. <https://doi.org/10.1080/10789669.1999.10391226>.
- ASTM International. ASTM D 4611: standard test method for specific heat of rock and soil. 2016.
- ASTM International. ASTM D5334-22a: standard test method for determination of thermal conductivity of soil and soft rock by thermal needle probe procedure. 2023.
- Bentz DP. Transient plane source measurements of the thermal properties of hydrating cement pastes. *Mater Struct*. 2007;40:1073–80. <https://doi.org/10.1617/s11527-006-9206-9>.
- Berkas I, Nejad Ghafar A, Fontana P, Caputcu A, Menciloglu Y, Saner Okan B. Synergistic effect of expanded graphite-silane functionalized silica as a hybrid additive in improving the thermal conductivity of cementitious grouts with controllable water uptake. *Energies*. 2020;13:3561. <https://doi.org/10.3390/en13143561>.
- Blázquez CS, Martín AF, Nieto IM, García PC, Sánchez Pérez LS, González-Aguilera D. Analysis and study of different grouting materials in vertical geothermal closed-loop systems. *Renew Energy*. 2017;114:1189–200. <https://doi.org/10.1016/j.renene.2017.08.011>.
- Bullard JW, Jennings HM, Livingston RA, Nonat A, Scherer GW, Schweitzer JS, Scrivener KL, Thomas JJ. Mechanisms of cement hydration. *Cem Concr Res*. 2011;41:1208–23. <https://doi.org/10.1016/j.cemconres.2010.09.011>.
- Delaleux F, Py X, Olives R, Dominguez A. Enhancement of geothermal borehole heat exchangers performances by improvement of bentonite grouts conductivity. *Appl Therm Eng*. 2012;33–34:92–9. <https://doi.org/10.1016/j.applthermaleng.2011.09.017>.
- Deutsche Norm. DIN 4127: Erd- und Grundbau—Prüfverfahren für Stützflüssigkeiten im Schlitzwandbau und für deren Ausgangsstoffe. 2014.
- Deutsche Norm. DIN EN ISO 17892-2: Geotechnische Erkundung und Untersuchung—Laborversuche an Bodenproben—Teil 2: Bestimmung der Dichte des Bodens (ISO 17892-2:2014). 2015.
- Deutsche Norm. DIN EN 196-1: Prüfverfahren für Zement—Teil 1: Bestimmung der Festigkeit; Deutsche Fassung EN 196-1:2016. 2016a.
- Deutsche Norm. DIN ISO 17892-3: Geotechnische Erkundung und Untersuchung—Laborversuche an Bodenproben—Teil 3: Bestimmung der Korndichte (ISO 17892-3:2015, korrigierte Fassung 2015-12-15). 2016b.
- Deutsche Norm. Kunststoffe, Bestimmung der Wärmeleitfähigkeit und der Temperaturleitfähigkeit Teil 2: Transientes Flächenquellenverfahren (Hot-Disk-Verfahren) (ISO/DIS 22007-2:2021. 2021a.
- Deutsche Norm. DIN EN ISO 11357-4: Kunststoffe—Dynamische Differenzkalorimetrie (DSC)—Teil 4: Bestimmung der spezifischen Wärmekapazität (ISO 11357-4:2021). 2021b.

- Deutsche Norm. DIN EN ISO 17892-1: Geotechnische Erkundung und Untersuchung—Laborversuche an Bodenproben—Teil 1: Bestimmung des Wassergehalts (ISO 17892-1:2014 + Amd 1:2022). 2022.
- Dils J, De Schutter G, Boel V. Influence of mixing procedure and mixer type on fresh and hardened properties of concrete: a review. *Mater Struct*. 2012;45:1673–83. <https://doi.org/10.1617/s11527-012-9864-8>.
- Do TM, Kim Y, Dang MQ. Influence of curing conditions on engineering properties of controlled low strength material made with cementless binder. *KSCE J Civ Eng*. 2017;21:1774–82. <https://doi.org/10.1007/s12205-016-0731-y>.
- Dong S, Liu G, Zhan T, Yao Y, Ni L. Performance study of cement-based grouts based on testing and thermal conductivity modeling for ground-source heat pumps. *Energy Build*. 2022;272:112351. <https://doi.org/10.1016/j.enbuild.2022.112351>.
- Erol S, François B. Efficiency of various grouting materials for borehole heat exchangers. *Appl Therm Eng*. 2014;70:788–99. <https://doi.org/10.1016/j.applthermaleng.2014.05.034>.
- Extremera-Jiménez AJ, Eliche-Quesada D, Guitérrez-Montes C, Cruz-Peragón F. Experimental work over borehole filling material to reinforce characterization and model validation of ground heat exchangers. *REPQJ*. 2021;19:109–14. <https://doi.org/10.24084/repqj19.227>.
- Fraç M, Szudek W, Szoldra P, Pichór W. Grouts with highly thermally conductive binder for low-temperature geothermal applications. *Constr Build Mater*. 2021;295:123680. <https://doi.org/10.1016/j.conbuildmat.2021.123680>.
- Gustafsson SE. Transient plane source techniques for thermal conductivity and thermal diffusivity measurements of solid materials. *Rev Sci Instrum*. 1991;62:797–804. <https://doi.org/10.1063/1.1142087>.
- Haines PJ, editor. Principles of thermal analysis and calorimetry. Cambridge: Royal Society of Chemistry; 2002.
- Höhne GWH, Hemminger WF, Flammersheim HJ, editors. Differential scanning calorimetry. Berlin Heidelberg: Springer; 2003.
- IEA ECES. Quality management in design, construction and operation of borehole systems. IEA Technology Collaboration Programme on Energy Conservation through Energy Storage (IEA ECES). 2020.
- ISO IEC 98-3. Uncertainty of measurement—Part 3: guide to the expression of uncertainty in measurement (GUM:1995). 2008.
- Javadi H, Mousavi Ajarostaghi S, Rosen M, Pourfallah M. A comprehensive review of backfill materials and their effects on ground heat exchanger performance. *Sustainability*. 2018;10:4486. <https://doi.org/10.3390/su10124486>.
- Kim D, Kim G, Kim D, Baek H. Experimental and numerical investigation of thermal properties of cement-based grouts used for vertical ground heat exchanger. *Renew Energy*. 2017;112:260–7. <https://doi.org/10.1016/j.renene.2017.05.045>.
- Kim D, Oh S. Relationship between the thermal properties and degree of saturation of cementitious grouts used in vertical borehole heat exchangers. *Energy Build*. 2019;201:1–9. <https://doi.org/10.1016/j.enbuild.2019.07.017>.
- Kim D, Oh S. Measurement and comparison of thermal conductivity of porous materials using box, dual-needle, and single-needle probe methods—a case study. *Int Commun Heat Mass Transfer*. 2020;118:104815. <https://doi.org/10.1016/j.icheatmasstransfer.2020.104815>.
- Kurdowski W. Cement and concrete chemistry. New York: Springer; 2014.
- Lafhaj Z, Goueygou M, Djerbi A, Kaczmarek M. Correlation between porosity, permeability and ultrasonic parameters of mortar with variable water/cement ratio and water content. *Cem Concr Res*. 2006;36:625–33. <https://doi.org/10.1016/j.cemconres.2005.11.009>.
- Li M, Zhang L, Liu G. Estimation of thermal properties of soil and backfilling material from thermal response tests (TRTs) for exploiting shallow geothermal energy: sensitivity, identifiability, and uncertainty. *Renew Energy*. 2019;132:1263–70. <https://doi.org/10.1016/j.renene.2018.09.022>.
- Mahmoud M, Ramadan M, Pullen K, Abdelkareem MA, Wilberforce T, Olabi A-G, Naher S. A review of grout materials in geothermal energy applications. *Int J Thermofluids*. 2021;10:100070. <https://doi.org/10.1016/j.ijft.2021.100070>.
- Marshall AK. The thermal properties of concrete. *Build Sci*. 1972. [https://doi.org/10.1016/0007-3628\(72\)90022-9](https://doi.org/10.1016/0007-3628(72)90022-9).
- Mascarin L, Garbin E, Di Sipio E, Dalla Santa G, Bertermann D, Artioli G, Bernardi A, Galgaro A. Selection of backfill grout for shallow geothermal systems: materials investigation and thermo-physical analysis. *Constr Build Mater*. 2022;318:125832. <https://doi.org/10.1016/j.conbuildmat.2021.125832>.
- Nian Y-L, Cheng W-L. Analytical g-function for vertical geothermal boreholes with effect of borehole heat capacity. *Appl Therm Eng*. 2018;140:733–44. <https://doi.org/10.1016/j.applthermaleng.2018.05.086>.
- Park M, Min S, Lim J, Choi JM, Choi H. Applicability of cement-based grout for ground heat exchanger considering heating-cooling cycles. *Sci China Technol Sci*. 2011;54:1661–7. <https://doi.org/10.1007/s11431-011-4388-y>.
- Pascual-Muñoz P, Indacochea-Vega I, Zamora-Barraza D, Castro-Fresno D. Experimental analysis of enhanced cement-sand-based geothermal grouting materials. *Constr Build Mater*. 2018;185:481–8. <https://doi.org/10.1016/j.conbuildmat.2018.07.076>.
- Prinz H, Strauß R. *Ingenieurgeologie*. Berlin Heidelberg: Springer; 2018.
- Schutter G, Taerwe L. Specific heat and thermal diffusivity of hardening concrete. *Mag Concr Res*. 1995. <https://doi.org/10.1680/mac.1995.47.172.203>.
- Shafiqh P, Asadi I, Akhiani AR, Mahyuddin NB, Hashemi M. Thermal properties of cement mortar with different mix proportions. *Mater Constr*. 2020;70:224. <https://doi.org/10.3989/mc.2020.09219>.
- Song X, Zheng R, Li R, Li G, Sun B, Shi Y, Wang G, Zhou S. Study on thermal conductivity of cement with thermal conductive materials in geothermal well. *Geothermics*. 2019;81:1–11. <https://doi.org/10.1016/j.geothermics.2019.04.001>.
- Stark J, Wicht B. *Dauerhaftigkeit von Beton*. Berlin Heidelberg: Springer; 2013.
- Verein Deutscher Ingenieure. VDI 4640, part 2: thermal use of the underground, Ground source heat pump systems. 2019.
- Verein Deutscher Zementwerke e.V. *Zement-Taschenbuch*. Erkrath. 2002.
- Viccaro M. Doped bentonitic grouts for implementing performances of low-enthalpy geothermal systems. *Geotherm Energy*. 2018. <https://doi.org/10.1186/s40517-018-0090-7>.
- Wang C, Fang H, Wang X, Lu J, Sun Y. Study on the influence of borehole heat capacity on deep coaxial borehole heat exchanger. *Sustainability*. 2022;14:2043. <https://doi.org/10.3390/su14042043>.

- Zhao D, Qian X, Gu X, Jajja SA, Yang R. Measurement techniques for thermal conductivity and interfacial thermal conductance of bulk and thin film materials. *J Electron Packag*. 2016. <https://doi.org/10.1115/1.4034605>.
- Zhao J, Huang G, Guo Y, Feng Z, Gupta R, Liu WW. Development of a novel cement-based grout with enhanced thermal and sealing performance for borehole heat exchangers. *Energy Build*. 2024;302:113754. <https://doi.org/10.1016/j.enbuild.2023.113754>.
- Zhou Y, Zhang Y, Xu Y. Influence of grout thermal properties on heat-transfer performance of ground source heat exchangers. *Sci Technol Built Environ*. 2018;24:461–9. <https://doi.org/10.1080/23744731.2017.1402645>.

Publisher's Note

Springer Nature remains neutral with regard to jurisdictional claims in published maps and institutional affiliations.